

# Evaluation of $^{99}\text{Mo}$ production in a small modular thorium based molten salt reactor

Xuzhong Kang<sup>a,b</sup>, Guifeng Zhu<sup>a,\*</sup>, Rui Yan<sup>a,b</sup>, Yafen Liu<sup>a</sup>, Yang Zou<sup>a,b</sup>, Ye Dai<sup>a</sup>, Xiangzhou Cai<sup>a,b</sup>

<sup>a</sup> Shanghai Institute of Applied Physics, Chinese Academy of Sciences, Shanghai, 201800, China

<sup>b</sup> University of Chinese Academy of Sciences, Beijing, 100049, China

## ARTICLE INFO

### Keywords:

Molten salt reactor  
 $^{99}\text{Mo}$   
 Fission yield  
 Migration  
 Off-gas module

## ABSTRACT

Producing medical radionuclide  $^{99}\text{Mo}$  in molten salt reactors is a very attractive choice to solve its global shortage. In this study, we evaluated the yield of  $^{99}\text{Mo}$  in the small modular thorium based molten salt reactor (SM-MSR). Firstly, the fuel burn-up analysis of SM-MSR was carried out by an in-house developed code (MOBAT), which takes the unique characteristics of molten salt reactor into account, and the variation of fission yield of  $^{99}\text{Mo}$  with burn-up time was obtained. The minimum value of the fission yield of  $^{99}\text{Mo}$  is  $1.13 \times 10^{-3}$  (6-day TBq/MW/s) at approximately 600 equivalent full power day. Then, based on the behavior of noble metals in the fuel salt and the experimental results of MSRE gas sample composition measurements,  $^{99}\text{Mo}$  migration probability from the primary loop to the off-gas module with the burn-up time was calculated, and the equilibrium value of the migration probability is obtained as 18.4%. When the load factor of SM-MSR is 0.75 (300 MWth), the annual  $^{99}\text{Mo}$  amount of migration to the off-gas module would be  $1.96 \times 10^6$  (6-day TBq) under the most conservative calculation. Finally, a filter system was added in the off gas module, and  $^{99}\text{Mo}$  would be extracted from the off gas. As long as the utilization percentage of  $^{99}\text{Mo}$  in the off gas module can reach 0.94%, the global demand under current data could be met, which implies a huge additional economic value for the SM-MSR.

## 1. Introduction

In nuclear medicine, radionuclide  $^{99\text{m}}\text{Tc}$  ( $T_{1/2} \approx 6$  h) is used for the detection of disease, for the study of organ structure and function, and for implementation in other important medical applications (Michael, 2018). Among the medical radioisotopes,  $^{99\text{m}}\text{Tc}$  occupies 80% of noninvasive nuclear diagnostic imaging of various organs all over the world (IAEA, 1999).  $^{99}\text{Mo}$  ( $T_{1/2} \approx 66$  h) is the main raw material of  $^{99}\text{Mo}/^{99\text{m}}\text{Tc}$  generator, and its production stability directly determines the supply of  $^{99\text{m}}\text{Tc}$ . The annual global demand for  $^{99}\text{Mo}$  was about 18,500 (6-day TBq) at present (WNA, 2019). However, the number of irradiation and processing facilities for  $^{99}\text{Mo}$  production over the world are very limited. Furthermore, most of them are aging, and many problems are emerging, such as supply chain withdrawal, reaction target changes and shutdowns for maintenance (Zou et al., 2016). All of them would lead to a serious shortage of  $^{99}\text{Mo}$  supply worldwide in the future. In addition, highly enriched uranium material required by the most of

the existing irradiation devices would cause the risk of nuclear proliferation. In order to handle the above challenges, the U.S. Department of Energy made a  $^{99}\text{Mo}$  production plan in February 2019 (DOE, 2019), and the evaluation of relevant commercial cooperation applications has been completed.

At present,  $^{99}\text{Mo}$  is produced by the irradiated target in a solid-fuel nuclear reactor, including neutron activation method  $^{98}\text{Mo} (n, \gamma) ^{99}\text{Mo}$  and fission method  $^{235}\text{U} (n, f) ^{99}\text{Mo}$  (Deng et al., 2006). Due to the different production principles of the two methods, the yield and specific activity of  $^{99}\text{Mo}$ , the volume of  $^{99}\text{Mo}/^{99\text{m}}\text{Tc}$  generator and production efficiency are different. Compared with the neutron activation method, the  $^{99}\text{Mo}$  produced by the fission method has a larger yield, higher specific activity, smaller volume of  $^{99}\text{Mo}/^{99\text{m}}\text{Tc}$  generator and higher efficiency. Therefore, the fission method is most widely used in the world. However, the fission method also has obvious disadvantages. (1)  $^{99}\text{Mo}$  generated by the fuel element in the reactor can't be utilized; (2) only a very small proportion of the  $^{235}\text{U}$  in the irradiated target are used;

\* Corresponding author.

E-mail addresses: [zhuguifeng@sinap.ac.cn](mailto:zhuguifeng@sinap.ac.cn), [zhuguifeng@sinap.ac.cn](mailto:zhuguifeng@sinap.ac.cn) (G. Zhu), [caixz@sinap.ac.cn](mailto:caixz@sinap.ac.cn) (X. Cai).

<https://doi.org/10.1016/j.pnucene.2020.103337>

Received 13 July 2019; Received in revised form 21 February 2020; Accepted 20 March 2020

Available online 8 April 2020

0149-1970/© 2020 Elsevier Ltd. All rights reserved.

(3) the gases, liquid and solid of waste are greatly generated; (4) the cost is also high.

In order to overcome the shortcomings of  $^{99}\text{Mo}$  production by the target, the concept of medical isotope production reactor (MIPR) was put forward by Ball (1992). The fuel used in MIPR is  $\text{UO}_2(\text{NO}_3)_2$  or  $\text{UO}_2\text{SO}_4$  homogeneous liquid, in which processes of target manufacturing, irradiation and dissolution are not required, and  $^{99}\text{Mo}$  can be directly extracted from homogeneous liquid fuel in the loop for processing and treatment. The technology based on the homogeneous liquid nuclear fuel possesses a number of obvious advantages in comparison with the “target” method (Chuvilin et al., 2012): (1) Nuclear nonproliferation; (2) High efficiency; (3) The utilization rate of  $^{235}\text{U}$  is high and the wastes are much less; (4) High economy: MIPR does not need target manufacture. Compared with traditional methods, the cost of  $^{235}\text{U}$  consumption and waste disposal in MIPR are only 0.36% and 2% by producing the same amount of  $^{99}\text{Mo}$ , respectively (Glenn and Heger, 1997).

The molten salt reactor using fuel both as coolant also has above advantages of homogeneous liquid reactor, and moreover, it has other characteristics:

- (1)  $^{99}\text{Mo}$  could be extracted online: As a result of fission,  $^{99}\text{Mo}$  is generated in the molten salt, then moves to the salt-gas border and passes to the gas phase space above the molten salt surface in form of fluorides and aerosols (Chuvilin et al., 2012). The gas phase space is connected to the off-gas system. Many molybdenum were found in the gas sample of pump bowl and the off gas system of MSRE (Kedl, 1972). These indicate that  $^{99}\text{Mo}$  could be extracted online by use of the off gas.
- (2) High production efficiency: compared with MIPR, molten salt reactor has no limitations associated with the power of the reactor (Chuvilin and Zagryadskii, 2009).
- (3) Extra profit: The molten salt reactor used for power generation can generate additional benefits by extracting and utilizing  $^{99}\text{Mo}$ , and the extraction method does not need to change the structure of the reactor body and hence does not affect the operation of the reactor itself.

From the above, it can be concluded that R&D of radionuclide (such as  $^{99}\text{Mo}$ ) extraction from molten salt fuel is very attractive. Chuvilin and Zagryadskii (2009) proposed to study  $^{99}\text{Mo}$  production in a solid-fuel reactor IR-8, in which one fuel element in the core was replaced by an auxiliary-loop facility filled with molten-salt fuel ( $66\text{LiF}-33.9\text{BeF}_2-0.1\text{UF}_4$ ,  $^{235}\text{U}:90$  wt%) and attached to the gas loop. The  $^{99}\text{Mo}$  produced by fission in the loop along with bubbles were migrated to the gas phase on the surface of the fuel salt and finally was collected. However, high-enriched uranium was used in their study, which is not conducive to prevent nuclear proliferation. The auxiliary-loop facility flows through the core of the solid fuel reactor may exert an impact on the safety, control and shielding of the reactor. The “target” was limited to the uranium in the loop rather than the uranium of the whole reactor, hence the yield of  $^{99}\text{Mo}$  was limited. The calculation of Sheu and Chao (2014) with SCALE software showed that the yield of  $^{99}\text{Mo}$  would be greatly enhanced if the uranium of the whole reactor in the molten salt reactor was treated as the ‘target’. However, they were limited to core calculations and were not involved in  $^{99}\text{Mo}$  migration.

In this study, considering the probability of  $^{99}\text{Mo}$  migration from the primary loop to the off-gas module, we evaluated the amount of  $^{99}\text{Mo}$  that can be utilized in SM-MSR. Section 2 includes a brief introduction to SM-MSR and the migration process of  $^{99}\text{Mo}$  produced from fuel salt fission in SM-MSR. Section 3 is the calculation of the  $^{99}\text{Mo}$  yield in SM-MSR core. Section 4 contains the  $^{99}\text{Mo}$  distribution in the primary loop and the probability of migration from the primary loop to off gas module. Section 5 shows the feasibility of  $^{99}\text{Mo}$  utilization in off gas module, and section 6 is the summary of this paper.

**Table 1**

Main parameters of small modular molten salt reactor.

parameter	value
Power	400 MWth
Fuel salt	$\text{LiF}-\text{BeF}_2-\text{UF}_4-\text{ThF}_4$
U-235 enrichment	19.75%
Salt working temperature	600–700 °C
Graphite moderator	Hexagonal blocks
Pump	Centrifugal structure
Gas separation mode	Spraying and bubbling
Heat exchanger	Shell-and-tube

## 2. SM-MSR and $^{99}\text{Mo}$ production

SM-MSR is a small-sized and modularized multi-purpose thorium based molten salt demonstration reactor proposed by TMSR (TMSR, 2016; Kang et al., 2018; Zhu et al., 2019a; Tan et al., 2019). It can be applied in power generation, seawater desalination, supply of super-critical steam for industrial use, hydrogen production, and the production of medical radionuclides.

The SM-MSR adopts fluorine salt ( $\text{LiF}-\text{BeF}_2-\text{UF}_4-\text{ThF}_4$ ) as fuel, with 19.75% enriched  $^{235}\text{U}$ , and graphite as moderation. The thermal power of SM-MSR is 400 MWth. The fissions occur in the reactor core, and fission heat is taken into heat exchanger by fuel salt itself driven by fuel pump. Most of fission products can be dissolved in fuel salt, whereas some noble gases and insoluble metals will be removed by bubbles circulating the loop. Main parameters of small modular molten salt reactor are listed in Table 1.

Molybdenum is produced by  $^{235}\text{U}$ ,  $^{233}\text{U}$  and  $^{239}\text{Pu}$  fission in SM-MSR. In fact, molybdenum behavior in molten salts is not well understood (Grimes et al., 1966; Rosenthal et al., 1967, 1968; Rosenthal et al., 1969a; Rosenthal et al., 1969b; Rosenthal et al., 1970a; Rosenthal et al., 1970b; Stoddard et al., 2019). It is found that Molybdenum mainly exists in the form of metallic and fluoride state in molten salt, but there are some ionic states. According to the general analysis in this paper, we considered that the fragment molybdenum exists in the fuel salt in form of salt-soluble ions, and these ions would become insoluble metallic atom very quickly, and then some of the atoms can enter into the gas phase as fluorides and aerosols.

$^{99}\text{Mo}$  will decay, be activated or dissolved in molten salt (very little), the rest of them would deposit on the surface of graphite and alloys, and adhere to the liquid-vapor interface (equivalent to deposit in the bubbles). The  $^{99}\text{Mo}$  generation and migration in SM-MSR are shown in Fig. 1. During the operation of SM-MSR, fission gas (Xe and Kr) and noble metal (Se, Nb, Mo, Tc, Ru, Rh, Pd, Ag, Sb and Te) are removed online by helium bubbles method. That is, helium bubbles are filled into molten salt from the pump bowl, and then pass through the heat exchanger, the core, and finally return to the pump bowl. The fission gas would diffuse into the helium bubbles (Kohn, 1968; Guo and Ji, 2017), while the noble metals would enter the helium bubbles and attach to the liquid-gas interface (Journee, 2014). As the fuel salt flows, the fission gas and noble metal would enter the pump bowl. In the pump bowl, the impingement of the jets from the spray ring generates large quantities of bubbles and froths, and this process is accompanied by the generation of salt mist which is highly concentrated in noble metals. This mist would migrate into the off gas module. The collection, cooling, separation, adsorption, filtration, purification, isotope separation and other physicochemical processes of the mist could extract the radioactive medical nuclide, such as  $^{99}\text{Mo}$ ,  $^{131}\text{I}$ ,  $^{89}\text{Sr}$ .

## 3. Calculation of the $^{99}\text{Mo}$ yield in SM-MSR

During the operation, SM-MSR employs online fuel feeding, online removal of the fission gas and the noble metals. The burn-up code of the traditional reactor can't be suitable for molten salt reactor calculation obviously. Based on these unique features of molten salt reactor, TMSR

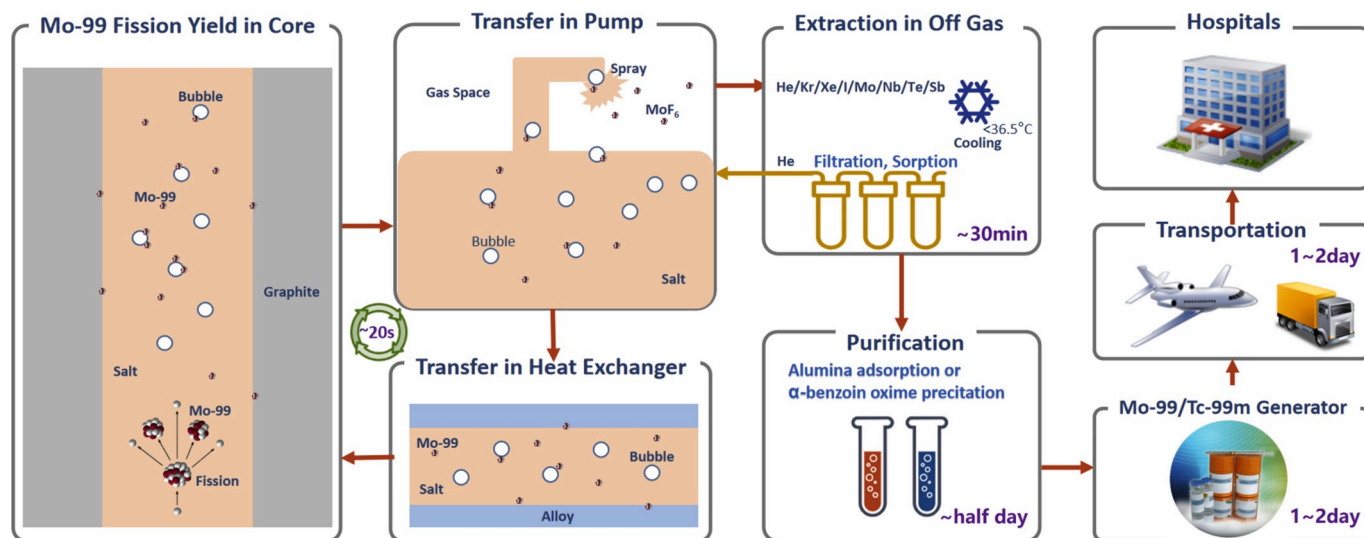


Fig. 1. Schematic diagram of  $^{99}\text{Mo}$  generation and migration in SM-MSR.

developed the code of MOBAT (Zhu et al., 2019b; Zhu et al., 2019c). It is a burn-up code coupled by MCNP and ORIGEN. The basic idea of the coupling is to use MCNP to calculate the neutron flux, power and one group cross section of each burn-up region as input parameters of ORIGEN. Running ORIGEN with given time step, the calculated nuclide components of each burn-up region are returned to MCNP, the coupling calculation in one time step is completed. MOBAT related program could control the amount of fuel nuclides added at each time step and removal fission products according to the needs of users.

In the burn-up calculation, we set the program to add fuel nuclides when the  $k_{\text{eff}}$  is less than 1, with the goal of maintaining the criticality of the core with reasonably minimal excess reactivity. We calculated the case of adding fuel without removing fission products in the fuel salt. The calculated amount of  $^{99}\text{Mo}$  in the SM-MSR varied with the burn-up time is shown in Fig. 2. The production of  $^{99}\text{Mo}$  and its decay reach an equilibrium state after approximately 20 days, the equilibrium value is approximately 408 (6-day TBq/MW). Since the  $^{235}\text{U}$  fission plays a major role in the generation of  $^{99}\text{Mo}$  in the initial stage of burn-up, the calculated results are the same as those calculated by SCALE (Sheu and Chao, 2014).

There are some differences of  $^{99}\text{Mo}$  cumulative yields in the fissile nuclides (NNDC, 2005; IAEA, 2008), see Table 2. As the burn-up deepens, fission contributions from  $^{233}\text{U}$  and  $^{239}\text{Pu}$  will increase since the amount of thorium is 6 times that of uranium in the initial loading of

Table 2

The thermal cumulative fission yields of  $^{99}\text{Mo}$  (NNDC, 2005; IAEA, 2008).

Nuclide	$^{233}\text{U}$	$^{235}\text{U}$	$^{239}\text{Pu}$
Fission yields	5.030%	6.132%	6.185%

SM-MSR. Therefore, the averaged cumulative yield of  $^{99}\text{Mo}$  will be varied with burn-up time.

In order to obtain the averaged cumulative fission yield of  $^{99}\text{Mo}$  varied with the burn-up time in the case of adding fuel and removing noble fission products in SM-MSR. The  $^{233}\text{U}$ ,  $^{235}\text{U}$  and  $^{239}\text{Pu}$  fission percentages varied with the burn-up time are calculated and shown in Fig. 3. As can be seen, the fission percentage of  $^{235}\text{U}$  rapidly decreases at the beginning of life and then increases slowly, while the fission percentage of  $^{233}\text{U}$  ascends quickly and then gently descents since the consumption of thorium, and the fission percentage of  $^{239}\text{Pu}$  can reach up to 40%. Therefore, the averaged cumulative fission yield of  $^{99}\text{Mo}$  reaches its lowest point at approximately 600 days, as shown in Fig. 3. The minimum value of the averaged cumulative fission yield of  $^{99}\text{Mo}$  is about

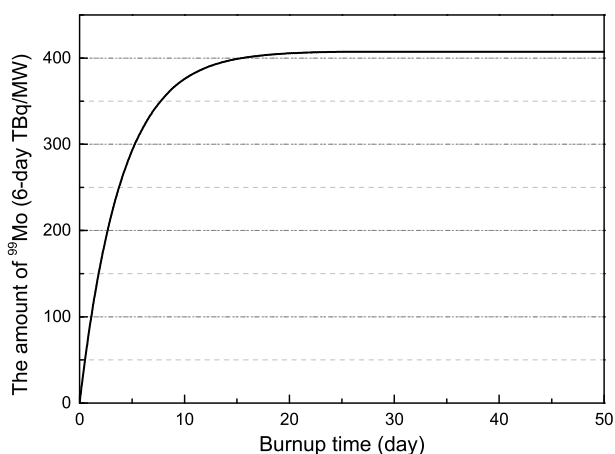


Fig. 2. The amount of  $^{99}\text{Mo}$  in SM-MSR varied with burn-up time in case of adding fuel without removing fission products at the beginning of life.

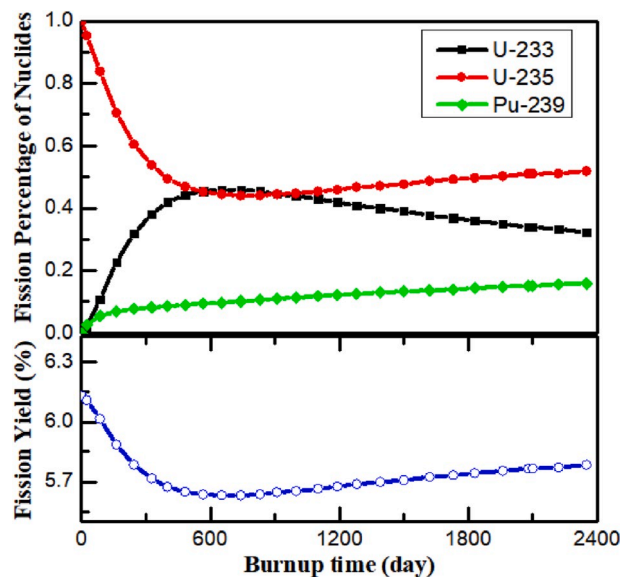


Fig. 3. Fission percentages of U-233, U-235 and Pu-239 and the fission yield of  $^{99}\text{Mo}$  varied with burn-up time in SM-MSR.

**Table 3**  
Parameters and corresponding values in SM-MSR calculation.

parameter	value
$\lambda$	$2.92 \times 10^{-6}/s$
$V$	$2.3 \times 10^7 cm^3$
$h^{gr}$	$5.33 \times 10^{-4} cm/s$
$A^{gr}$	$2.61 \times 10^6 cm^2$
$h^{he}$	$4.66 \times 10^{-3} cm/s$
$A^{he}$	$1.97 \times 10^7 cm^2$
$h^r$	$1.04 \times 10^{-2} cm/s$
$A^r$	$4.0 \times 10^5 cm^2$
$h^b$	$4.23 \times 10^{-2} cm/s$
$A^b$	$2.17 \times 10^6$ to $6.51 \times 10^7 cm^2$

5.64%, and the corresponding production rate of  $^{99}Mo$  is  $1.13 \times 10^{-3}$  (6-day TBq/MW/s).

#### 4. The migration probability of $^{99}Mo$ from primary loop to off gas module

As introduced above,  $^{99}Mo$  is reduced to metals in the fuel salt, and it would migrate to the surface of alloy, the surface of graphite and liquid-gas interfaces. In order to obtain the  $^{99}Mo$  migration probability from the primary loop to the off-gas module, the noble metal migration model (Kedl, 1972) was used for calculation. The equilibrium equation of  $^{99}Mo$  in the fuel salt is as follows:

$$V \frac{dC^s(t)}{dt} = y(t)p - \lambda VC^s(t) - h^{gr}A^{gr}C^s(t) - h^{he}A^{he}C^s(t) - h^rA^rC^s(t) - h^bA^bC^s(t) \quad (1)$$

where, the first terms in the right of equation (1) are  $^{99}Mo$  sources from cumulative fission (including direct fission and decay). The rest are disappearance terms, which in turn are  $^{99}Mo$  decay rate in salt, deposition rate on graphite, deposition rate on heat exchanger, deposition rate on rest of fuel loop (fuel loop piping, core and pump volute, pump impeller, core support grid, etc.) and deposition rate on liquid-gas interfaces, respectively.  $C^s(t)$  is the concentration of  $^{99}Mo$  in fuel salt at the burn-up time  $t$  (6-day TBq/cm<sup>3</sup>);  $V$  is the volume of fuel salt in fuel loop (cm<sup>3</sup>);  $t$  is the burn-up time (s);  $y(t)$  is the cumulative fission production rate of  $^{99}Mo$  at the burn-up time  $t$  (6-day TBq/MW/s), the value can be obtained from Fig. 3;  $P$  is the SM-MSR power level (MW);  $\lambda$  is the decay constant of  $^{99}Mo$  (1/s);  $h^{gr}$  is the mass transfer coefficient to graphite in SM-MSR core (cm/s);  $h^{he}$  is the mass transfer coefficient to primary heat exchanger (cm/s);  $h^r$  is the mass transfer coefficient to rest of loop (cm/s);  $h^b$  is the mass transfer coefficient to circulating bubbles (cm/s);  $A^{gr}$  is the surface area of graphite exposed to fuel salt (cm<sup>2</sup>);  $A^{he}$  is the total surface area of alloy in heat exchanger exposed to fuel salt (cm<sup>2</sup>);  $A^r$  is the surface area of rest of loop exposed to fuel salt (cm<sup>2</sup>);  $A^b$  is the surface area of circulating bubbles (cm<sup>2</sup>).

The surface areas of graphite, primary heat exchanger and rest of loop in SM-MSR are listed in Table 3. However, the surface area of bubbles may have a significant change according to the operation condition. In MSRE, the volume fraction of bubbles circulating with the fuel salt was estimated to be in the range of 0.02 percent to 0.045 percent during the  $^{235}U$  operation, and in the range of 0.5 percent to 0.6 percent during the  $^{233}U$  operation (Robinson and Fry, 1969). The bubble diameter would be use a mean value of 0.0127 cm (Kedl, 1972). Therefore, according the salt volume, we infer that the surface area of bubbles in SM-MSR can be from  $2.17 \times 10^6$  to  $6.51 \times 10^7 cm^2$ .

The mass transfer coefficients will be evaluated by the heat transfer-mass transfer analogy, which is related with the hydraulic diameter  $d$ , speed  $v$ , density  $\rho$ , viscosity  $\mu$ , and diffusion coefficient  $D$ . it can be

**Table 4**  
 $^{99}Mo$  distribution in the primary loop of the SM-MSR and MSRE.

Deposition location	MSRE bubbles	MSRE bubbles	SM-MSR bubbles	SM-MSR bubbles
Heat exchanger	11.7%	0.7%	48.5%	3.2%
Graphite	6.2%	0.4%	0.8%	0.1%
Bubbles	68.0%	98.1%	48.5%	96.5%
Rest of fuel loop	14.1%	0.8%	2.2%	0.2%

obtained by equation (2). In this paper, the mass transfer coefficient to bubbles is referred from MSRE due to its similar bubbles behavior.

$$h = 0.023 \frac{D}{d} \left( \frac{\rho v}{\mu} \right)^{0.8} \left( \frac{\mu}{\rho D} \right)^{0.4} \quad (2)$$

Based on the coefficients in equation (1), we could get the  $^{99}Mo$  deposition rate on the different area in SM-MSR, and therefore  $^{99}Mo$  distribution in the primary loop could be obtained, as shown in Table 4. For comparison, the corresponding values for MSRE were also calculated. The  $^{99}Mo$  distribution in the primary loop of the SM-MSR and MSRE are different under the same bubble content, which is because the primary loop structure of SM-MSR is not simply amplified by the corresponding structure of MSRE. In addition, it can be seen directly from Table 4 that even in low volume fraction of bubbles content in SM-MSR, the migration probability of  $^{99}Mo$  into bubbles is up to 48.5%.

With the operation of SM-MSR, the calculated  $C^s(t)$  value using the migration model will reach saturation (or equilibrium) in about 20 min. The  $C^s(t)$  saturation concentration is  $1.7 \times 10^{-6}$  (6-day TBq/cm<sup>3</sup>) and the corresponding ratio of the total deposition (including deposition on the surface of heat exchanger, graphite, bubbles and rest of loop) is almost 1. The result is exactly the same as shown in Fig. 2 in the paper (Stoddard et al., 2019).

When in bubbles, the  $^{99}Mo$  will disappear by decay and migration to off gas. The equilibrium equation of  $^{99}Mo$  in the bubbles is as follows:

$$\frac{dI(t)}{dt} = h^b A^b C^s(t) - \lambda I(t) - Z I(t) \quad (3)$$

where,  $I(t)$  is the total amount of  $^{99}Mo$  in bubbles of SM-MSR fuel loop (6-day TBq);  $Z$  is the generalized rate constant of  $^{99}Mo$  migrating from bubbles to off gas module (1/s).

Supposing that the migration probability of  $^{99}Mo$  produced by fission from the primary loop to the off gas module with the burn-up time  $t$  is  $g(t)$ , we can obtain that

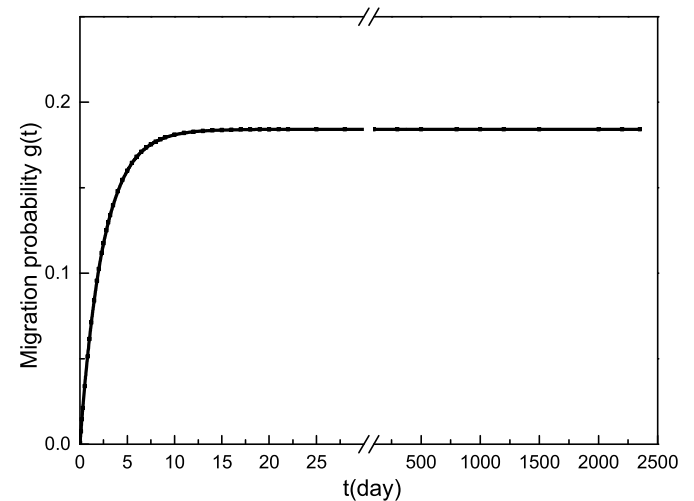


**Fig. 4.** The migration probability of  $^{99}Mo$  from the primary loop to the off gas module varies with the burn-up time in SM-MSR.

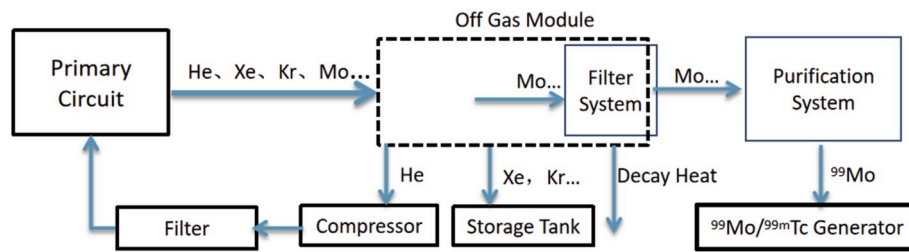


Fig. 5. Flowchart of  $^{99}\text{Mo}$  extraction.

$$g(t) = \frac{Zl(t)}{y(t)P} \quad (4)$$

By solving equations (1), (3) and (4), and suppose  $l(0) = 0, C^s(0) = 0$ , the equation of  $g(t)$  can be obtained. The migration probability  $g(t)$  isn't related to  $P$ , but closely related to the ratio of  $^{99}\text{Mo}$  deposited on gas-liquid interface, the surfaces of primary heat exchanger, graphite and rest of loop, respectively.

The value of  $Z$  is determined by many factors, such as the volume percentage of bubbles, the flow rate of fuel salt and the mechanical structures of the pump and off gas module. These factors are considered to be the same or similar to the corresponding ones of MSRE, thus the value of  $Z$  can be referred to the value of MSRE (Kedl, 1972) for the sake of simple calculation,  $Z = 2.78 \times 10^{-6}/\text{s}$ . In order to get a conservative estimate of  $g(t)$ , the value of  $A^b$  is assigned a minimum value  $2.17 \times 10^6 (\text{cm}^{-2})$ . The variation of migration probability  $g(t)$  of  $^{99}\text{Mo}$  from the primary loop to the off gas module with the burn-up time  $t$  is shown in Fig. 4.

Fig. 4 shows that the migration probability increases rapidly with the increase of time, and tends to be equilibrium after about 10 days where the maximum value is about 18.4%. If the load factor of SM-MSR is 0.75, the most conservative estimate amount of  $^{99}\text{Mo}$  produced by fission within one year is  $1.07 \times 10^7$  (6-day TBq). Therefore, we can get the annual amount of  $^{99}\text{Mo}$  migrated from the primary loop to the off gas module is  $1.96 \times 10^6$  (6-day TBq).

## 5. $^{99}\text{Mo}$ extraction in off gas module

The purpose of SM-MSR off gas module is to remove the fission gas and volatile fission products from the fuel salt, and to increase the neutron economy and thorium utilization. In the pump bowl, the off gas (helium, gaseous fission products and volatile fission products) is removed from the primary circuit and flows into the off gas module. The off gas would be cooled and decay in the off gas module, and the helium, xenon and krypton will be stored in their respective tanks after the separation process. The separated helium gas will be recycled by re-injecting into the gas supply system, which is expected to significantly reduce the cost resulted from helium gas consumption.

In order to extract  $^{99}\text{Mo}$  from off gas module (the flowchart of  $^{99}\text{Mo}$  extraction is shown in Fig. 5), a filtering system is added to the off gas module. Molybdenum fluoride and aerosols in the off gas module would be absorbed by the filtering system. The adsorbent of the filtering system can be NaF (Artyukhov et al., 2010; Li et al., 2014), and the adsorbent may be periodically withdrawn from the gas off module into purification system or other methods are adopted to take out the adsorbent. The adsorbent contain certain fission products, and the processes for isolating  $^{99}\text{Mo}$  from the adsorbent may adopt traditional methods. (1) Alumina adsorption: the dissolving adsorbent passes through an alumina column, which selectively absorbs  $^{99}\text{Mo}$  and radio-tellurium fission products. The alumina column is washed in multiple steps, and the  $^{99}\text{Mo}$  is eventually isolated (Stang, 1964). (2)  $\alpha$ -benzoin oxime precipitation: the  $^{99}\text{Mo}$  is selectively precipitated by adding  $\alpha$ -benzoin oxime (Arino et al., 1974).

The annual global demand for  $^{99}\text{Mo}$  is 18,500 (6-day TBq) at present

(WNA, 2019). The global consumption could be met as long as the utilization percentage of  $^{99}\text{Mo}$  in the off gas module of SM-MSR reaches 0.94%.

Of course, much research works are required to improve this initial study, including further analyze the amount of  $^{99}\text{Mo}$  migrated to each device in the off gas module; how to ensure the safely extraction of compounds containing  $^{99}\text{Mo}$  in the off gas module; and how to economically develop a process for purifying  $^{99}\text{Mo}$  from the compounds.

## 6. Summary

Molten salt reactor has great advantages in solving the problem of the global shortage of radioactive medical nuclides  $^{99}\text{Mo}$ . The  $^{99}\text{Mo}$  production in SM-MSR was evaluated in this study. The fission yield of  $^{99}\text{Mo}$  reaches its lowest point when the fission percentage of  $^{235}\text{U}$  reaches its maximum and the corresponding fission percentage of  $^{235}\text{U}$  reaches its minimum at approximately 600 days. The minimum value of the fission yield of  $^{99}\text{Mo}$  is about 5.64%, and the corresponding production rate of  $^{99}\text{Mo}$  is  $1.13 \times 10^{-3}$  (6-day TBq/MW/s). The variation of migration probability of the  $^{99}\text{Mo}$  from the primary loop to the off-gas module with the burn-up time was calculated based on the method introduced by Kedl (1972), the migration probability is about 18.4% under a 0.02% bubbles assumption and the generalized rate constant for migration from the bubble to the off gas module  $^{99}\text{Mo}$  is equal to  $2.78 \times 10^{-6}/\text{s}$ . The result of distribution may have some uncertainties since the insolubility of  $^{99}\text{Mo}$  in salt is still skeptical and some mass transfer coefficients was simply evaluated by the heat transfer-mass transfer analogy. Those work should be carried out in the future. When the load factor of SM-MSR is 0.75, the annual  $^{99}\text{Mo}$  amount of migration to the off-gas module is  $1.96 \times 10^6$  (6-day TBq). In order to extract medical radionuclide from off gas module, a filtering system was added.  $^{99}\text{Mo}$  would be absorbed by the filtering system through reasonable design of the relevant equipment in the off gas module and reasonably controlling the temperature and flow of the off gas in the equipment.

The global radioisotope market was valued at \$9.6 billion in 2016, with medical radioisotopes accounting for about 80% of this, and it is poised to reach about \$17 billion by 2021 (WNA, 2019). Utilization of medical radioisotopes in off gas module would make SM-MSR generating huge additional economic value.

## CRediT authorship contribution statement

**Xuzhong Kang:** Investigation, Data curation, Writing - original draft. **Guifeng Zhu:** Conceptualization, Methodology, Software. **Rui Yan:** Writing - review & editing. **Yafen Liu:** Writing - review & editing. **Yang Zou:** Funding acquisition. **Ye Dai:** Software, Resources. **Xiangzhou Cai:** Supervision.

## Acknowledgement

This paper is supported by the Chinese TMSR Strategic Pioneer Science and Technology Project (No.XDA02010000), the Frontier Science Key Program of Chinese Academy of Sciences (No.QYZDY-SSWJSC016), and the Shanghai Sailing Program (NO.Y931021031).

## Appendix A. Supplementary data

Supplementary data to this article can be found online at <https://doi.org/10.1016/j.pnucene.2020.103337>.

## References

- Arino, H., Kramer, H., McGovern, J., Thornton, A.K., 1974. Production of high purity fission product molybdenum-99. U.S. Patent 3, 799,883.
- Artyukhov, A.A., Kravets, Y.M., Seregin, M.B., et al., 2010. Transfer by metallic service lines and sorption extraction of MoF6 from the gas flow. *J. Eng. Phys. Thermophys.* 83 (2), 235–242.
- Ball, R.M., 1992. Testimony before the Congressional Committee on US Resources on the Production of 99Mo with Aqueous Homogeneous Reactors. Mike Synar, Chairman.
- Chuvilin, D.Y., Zagryadskii, V.A., 2009. New method of producing 99Mo in molten salt fluoride fuel. *Atom. Energy* 107 (3), 185–193.
- Chuvilin, D.Y., Khvostionov, V.E., Markovskij, D.V., et al., 2012. Low-Waste and Proliferation-Free Production of Medical Radioisotopes in Solution and Molten-Salt Reactors, Radioactive Waste, Dr. Rehab Abdel Rahman (Ed.), ISBN: 978-953-51-0551-0, InTech. Available from: <http://www.intechopen.com/books/radioactive-waste/low-waste-and-proliferation-free-production-of-medicalisotopes-in-solution-and-molten-salt-reactors>.
- Deng, Q., Li, M.L., Cheng, Z.Y., 2006. Application of <sup>99</sup>Mo production through medical isotope production reactor (MIPR). *Chinese Journal of Nuclear Science and Engineering* 26 (2), 165–167.
- DOE, 2019. Department of Energy to Negotiate Cooperative Agreements on the Production of Molybdenum-99 with Four U.S. Companies. <https://www.energy.gov/articles/department-energy-negotiate-cooperative-agreements-production-molybdenum-99-four-us>.
- Glenn, D., Heger, A.S., et al., 1997. Comparison of characteristics of solution and conventional reactors for 99Mo production. *Nucl. Technol.* 118 (2), 142–150.
- Grimes, W., Bohlmann, E., McDuffie, H., et al., 1966. Reactor Chemistry Division Annual Progress Report. ORNL-4076.
- Guo, C., Ji, R.M., et al., 2017. Xenon analysis of thorium molten salt experiment reactor-liquid fuel. *Nucl. Tech.* 40 (4).
- IAEA, 1999. Production Technologies for Molybdenum-99 and Technetium-99m. IAEA-TECDOC-1065, International Atomic Energy Agency, Vienna, Austria.
- IAEA, 2008. HANDBOOK OF NUCLEAR DATA FOR SAFEGUARDS: DATABASE EXTENSIONS, vol. 5. IAEA Nuclear Data Section, Wagramer Strasse, Vienna, Austria. A-1400. <https://www.nds.iaea.org/sgnucdat/c3.htm>.
- Journee, D., 2014. Helium Bubbling in a Molten Salt Fast Reactor (A Flotation Process). Delft University of Technology, Delft.
- Kang, X.Z., Zhu, G.F., Zou, Y., et al., 2018. Physical analysis of control rods arrangement in core of a small modular molten salt reactor. *Nucl. Power Eng.* 39 (5).
- Kedl, R.J., 1972. The Migration of a Class of Fission Products(Noble Metals)in the Molten-Salt Reactor Experiment. ORNL-TM-3884.
- Kohn, H.W., 1968. Bubbles, Drops, and Entrainment in Molten Salts. ORNL-TM-2373.
- Li, Y.J., Cheng, Z.Q., Zhang, H.Q., et al., 2014. A novel technique for preparation of the porous adsorbent NaF and a preliminary study on its adsorption capacity for MoF6. *Nucl. Tech.* 37 (8), 080601.
- Michael, A.B.N., 2018. The global impact of the Mo-99 shortage. *Biomed J Sci &Tech Res* 4 (5), 4172–4176.
- NNDC, 2005, <https://www.nndc.bnl.gov>. Library:JEFF-3.1.
- Robinson, J.C., Fry, D.N., 1969. Determination of the void fraction of the MSRE using small induced pressure perturbations, USEAC report ORNL-TM-2318. ORNL, Feb. 6.
- Rosenthal, M., Briggs, R., Haubenreich, P., 1970a. Molten-salt Reactor Program Semiannual Progress Report. ORNL-4622.
- Rosenthal, M., Briggs, R., Kasten, P., 1967. Molten-salt Reactor Program Semiannual Progress Report. ORNL-4191.
- Rosenthal, M., Briggs, R., Kasten, P., 1968. Molten-salt Reactor Program Semiannual Progress Report. ORNL-4254.
- Rosenthal, M., Briggs, R., Kasten, P., 1969a. Molten-salt Reactor Program Semiannual Progress Report. ORNL-4396.
- Rosenthal, M., Briggs, R., Kasten, P., 1969b. Molten-salt Reactor Program Semiannual Progress Report. ORNL-4449.
- Rosenthal, M., Briggs, R., Kasten, P., 1970a. Molten-salt Reactor Program Semiannual Progress Report. ORNL-4548.
- Sheu, R.J., Chao, C.C., et al., 2014. A fuel depletion analysis of the MSRE and three conceptual small molten-salt reactors for Mo-99 production. *Ann. Nucl. Energy* 71, 111–117.
- Stang, L.G., 1964. Manual of Isotope Production Processes in Use at Brookhaven. National Laboratory.
- Stoddard, M.N., Harb, J.N., Memmott, M.J., 2019. Numerical analysis of isotope production in molten salt reactors: a case study for Molybdenum-99 production. *Ann. Nucl. Energy* 129, 56–61.
- Tan, M.L., Zhu, G.F., Zou, Y., et al., 2019. Research on the effect of the heavy nuclei amount on the temperature reactivity coefficient in a small modular molten salt reactor. *NUCL SCI TECH* 30 (9), 140.
- TMSR, 2016. Report on Pre-conceptual Design of Small Modular Thorium Based Molten Salt Demonstration Reactor (Internal Report).
- WNA, 2019. Radioisotopes in Medicine (Updated February 2019). World Nuclear Association. <http://www.world-nuclear.org/>.
- Zhu, G.F., Zou, Y., Yan, R., et al., 2019a. Low enriched uranium and thorium fuel utilization under once-through and offline reprocessing scenarios in small modular molten salt reactor. *Int. J. Energy Res.* 1–13.
- Zhu, G.F., Liu, S.J., Zou, Y., et al., 2019b. Thorium utilization with pebble mixing system in fluoride salt-cooled High Temperature Reactor. *Prog. Nucl. Energy* 114, 84–90.
- Zhu, G.F., Yan, R., Dai, M., et al., 2019c. Monte Carlo burn-up code development based on multi-group cross section method. *Prog. Nucl. Energy* 110, 24–29.
- Zou, W., Yin, H.Y., Liu, Q., 2016. Survey on the supply of the fission 99Mo. *Chin J Nucl Med Mol Imaging* 36 (4), 375–377.